INTERNATIONAL JOURNAL OF
NUMERICAL ANALYSIS AND MODELING
Volume 9, Number 1, Pages 105–114

APPROXIMATE SIMILARITY SOLUTION TO A NONLINEAR DIFFUSION EQUATION WITH SPHERICAL SYMMETRY

JEFF MORTENSEN, SAYAKA OLSEN, JEAN-YVES PARLANGE, AND ALEKSEY S. TELYAKOVSKIY

Abstract. In this article we construct an approximate similarity solution to a nonlinear diffusion equation in spherical coordinates. In hydrology this equation is known as the Boussinesq equation when written in planar or cylindrical coordinates. Recently Li et al. [8] obtained an approximate similarity solution to the Boussinesq equation in cylindrical coordinates. Here we consider the same problem in spherical coordinates with the prescribed power law point source boundary condition. The resulting scaling function has a power law singularity at the origin versus a logarithmic singularity in the cylindrical case.

Key Words. approximate solutions, similarity solutions, Boussinesq equation, nonlinear diffusion.

1. Introduction

Nonlinear diffusion equations appear in many branches of natural sciences and there are multiple methods to solve them, see e.g. [5, 7]. The Boussinesq equation appearing in hydrology is an example of a diffusion equation with a linear diffusivity [4]. Some mathematical properties of this equation in planar, cylindrical and spherical cases are analyzed in [1]. It is shown there that for certain initial and boundary conditions the problem can be reduced to a boundary value problem for a nonlinear ordinary differential equation using similarity transformations. Here we consider the zero initial condition, so as shown in [3] the solutions propagate with the finite speed. An additional complexity of the problem is due to the existence of a free boundary that must be found during the solution process. We note that exact solutions exist only for a very limited number of values of the parameters describing the behavior at the boundary. As a result numerical or approximate analytical techniques must be employed to obtain the solution. Often Shampine's method [11] is used to solve these problems numerically. There are many approximate analytical methods of solution. We shall list only some of them. In the planar case you can construct approximate polynomial solutions that satisfy certain properties of the true solution of the differential equation [10, 13, 14]. In the cylindrical case there is a logarithmic singularity at the inlet, so an approximate similarity solution must include a logarithmic term [8]. In this article we construct an approximate similarity solution to the Boussinesq equation in spherical coordinates. For a comprehensive review of the literature on approximate analytical solutions for hydrologic applications see [12].

Our main goal is to expand the results of [8] from the cylindrical case to the spherical case. While [8] deals with the construction of approximate similarity

Received by the editors May 9, 2009 and, in revised form, October 21, 2009.

2000 *Mathematics Subject Classification.* 34B15, 35K20, 76S05, 80A20.

solution to the Boussinesq equation, here we use results of [1] to construct an approximate similarity solution when the Boussinesq equation is considered in the spherical setting and the flow is emanating from a point source. As emphasized in [1] only flux boundary conditions make physical sense.

The paper is structured as follows: In Section 2 we provide the mathematical formulation of the problem and obtain an approximate solution; In Section 3 we compare our approximate solution against the numerical solution; We summarize the findings in Section 4.

2. Theory

We consider the Boussinesq equation in the case of spherical symmetry

$$\theta_s \frac{\partial h}{\partial t} - \frac{K_s}{r^2}\frac{\partial}{\partial r}\left(r^2 h \frac{\partial h}{\partial r}\right) = 0, \tag{1}$$

where t is time and r is the distance from the point source. In hydrologic applications h is the pressure head, θ_s is the porosity and K_s is the conductivity. This equation also appears in nonlinear heat conduction (e.g. [15]) with the dependent variable being temperature.

A physically meaningful solution to this equation with specified flux at the origin is discussed in [1]. The case of a power-law flux (α in equations (2) and (3) below is a parameter related to the power) at the origin is special since it allows the reduction of (1) to a nonlinear ordinary differential equation. Using dimensional analysis analogous to Barenblatt's [1] and Li et al.'s [8] the following two groups of dimensionless variables can be formed

$$h = Mt^{\frac{2\alpha-3}{5}} f(\eta) \tag{2}$$

and

$$r = \eta N t^{\frac{\alpha+1}{5}}, \tag{3}$$

where f is a scaling function and η is a similarity variable. As in the cylindrical case [8], without loss of generality we can relate constants M and N by

$$MK_s = N^2\theta_s \tag{4}$$

and we can define N in terms of the position of the front r_0 where $h = 0$

$$r_0 = Nt^{\frac{\alpha+1}{5}} \tag{5}$$

which implies

$$f(1) = 0. \tag{6}$$

Substituting (2) and (3) into (1) we obtain an ordinary differential equation

$$\frac{\alpha+1}{5}\eta\frac{df}{d\eta} - \frac{2\alpha-3}{5}f + \frac{1}{\eta^2}\frac{d}{d\eta}\left(\eta^2 f \frac{df}{d\eta}\right) = 0. \tag{7}$$

The exact solution exists only for $\alpha = 0$. The solution propagates with finite speed as we can see from (5). This result was first obtained in [1] and later a more rigorous proof was provided in [3]. So far we have not imposed any conditions on α.

At the origin the boundary condition for the flux q is specified as

$$q = -K_s 4\pi r^2 h \frac{\partial h}{\partial r} \quad \text{at} \quad r = 0. \tag{8}$$

Using (2) and (3) the above can be rewritten as

$$q = -K_s 4\pi N M^2 t^{\alpha-1}\left[\eta^2 f \frac{df}{d\eta}\right]_{\eta=0}. \tag{9}$$

Since the integral $\int_0^t q d\bar{t}$ represents the total amount of substance injected into the system over time, it must be finite. In view of this and (9) we see that $\alpha > 0$.

Integration of equation (1) in space implies that

$$q = 4\pi\theta_s \int_0^{r_0} r^2 \frac{\partial h}{\partial t} dr. \tag{10}$$

Direct integration of equation (7) over η between zero and one results in

$$\left[\eta^2 f \frac{df}{d\eta}\right]_{\eta=0} = -\alpha \int_0^1 f\eta^2 d\eta. \tag{11}$$

We notice here the key difference in the change of variables (2,3) from the approach of Barenblatt [1, 2]. In Barenblatt's approach the position of the front η_0 is not known, while both quantities appearing in (11) are known. Here we fix the position of the front $\eta_0 = 1$, but as a result the second moment of f is no longer known. This is an inherent feature of a free boundary problem and this boundary must be found during the solution process.

Integrating (7) between η and 1 we obtain

$$\frac{df}{d\eta} + \frac{\alpha+1}{5}\eta = -\frac{\alpha}{f\eta^2} \int_\eta^1 f\bar{\eta}^2 d\bar{\eta}. \tag{12}$$

From the above we have

$$\frac{df}{d\eta} = -\frac{1+\alpha}{5} \quad \text{at} \quad \eta = 1. \tag{13}$$

Equation (7) with boundary conditions (6) and (13) at $\eta = 1$ represents a Cauchy problem that can be solved numerically. For example, a standard Runge-Kutta solver can be used to calculate the value of $f(\eta)$ for $0 < \eta \leq 1$. The Taylor series of f centered at $\eta = 1$ can be used to start the numerical calculation

$$f \sim \frac{\alpha+1}{5}(1-\eta) + \frac{3\alpha-2}{20}(1-\eta)^2 + \frac{(\alpha+2)\alpha}{\alpha+1}\frac{5}{72}(1-\eta)^3 + \cdots \tag{14}$$

2.1. Estimate of the front position. In order to construct the approximate solution we need to know the second moment of f, i.e., $\int_0^1 f\eta^2 d\eta$. In this section we obtain some approximate expressions for this moment. From equations (9) and (11) we have the cumulative flux

$$\int_0^t q d\bar{t} = Ct^\alpha, \tag{15}$$

where

$$C = K_s 4\pi N M^2 \int_0^1 f\eta^2 d\eta \tag{16}$$

and for the front position r_0, we have from Eqs. (4), (5) and (16)

$$r_0^5 = \frac{K_s t^{\alpha+1} C}{4\pi\theta_s^2 \int_0^1 f\eta^2 d\eta}, \tag{17}$$

so we need the second moment of f in order to find r_0.

From equation (12) we obtain the following asymptotic behavior as $\eta \to 0$

$$f^2 \sim \frac{2\alpha}{\eta} \int_0^1 f\eta^2 d\eta. \tag{18}$$

We can expand f in powers of α assuming that α is small

$$f \sim \frac{1}{10}(1-\eta^2) + \frac{2}{15}\left(\frac{1}{\eta} - 1 + \ln\frac{2}{\eta+1}\right)\alpha + \mathbf{f_2}(\eta)\frac{\alpha^2}{2} + \dots \tag{19}$$

The constant term in (19), viewed as a function of α, is the same as the constant term in (14). The expression for $\mathbf{f_2}(\eta)$ is provided in Appendix A and contains a dilogarithmic function (e.g. [9]). Using the first two terms of equation (19) we obtain

$$\int_0^1 f\eta^2 d\eta \sim \frac{1}{75} + \frac{8-6\ln 2}{135}\alpha. \tag{20}$$

A similar result ($\int_0^1 f\eta^2 d\eta \sim \frac{1}{75} + \frac{13}{600}\alpha$) can be obtained from the first two terms of equation (14).

The first three terms in equation (19) result in

$$\int_0^1 f\eta^2\, d\eta \sim \frac{1}{75} + \frac{8-6\ln 2}{135}\alpha + \frac{1}{135}\left(\frac{476}{9} - \frac{10}{3}\pi^2 + 20\ln^2 2 - \frac{152}{3}\ln 2\right)\frac{\alpha^2}{2}. \tag{21}$$

Considering the limit of equation (7) as $\alpha \to \infty$ it is possible to show that f is proportional to α. Hence, $\int_0^1 f\eta^2 d\eta$ is proportional to α also. So following [8] we express $\int_0^1 f\eta^2 d\eta$ as a continued-fraction approximation

$$\int_0^1 f\eta^2 d\eta \sim \frac{1}{75} + \frac{8-6\ln 2}{135}\alpha\left(\frac{1+A\alpha}{1+B\alpha}\right). \tag{22}$$

Next we obtain a relationship between A and B. Since for α near zero

$$\begin{aligned}(1+A\alpha)\frac{1}{1+B\alpha} &= (1+A\alpha)[1 - B\alpha + B^2\alpha^2 - B^3\alpha^3 + \cdots] \\ &= 1 + (A-B)\alpha - [AB - B^2]\alpha^2 + \cdots] \\ &= 1 + (A-B)\alpha + O(\alpha^2)\end{aligned}$$

the right side of (22) can be rewritten

$$\int_0^1 f\eta^2\, d\eta \approx \frac{1}{75} + \frac{8-6\ln 2}{135}\alpha[1 + (A-B)\alpha + O(\alpha^2)].$$

Comparing coefficients of α^2 between this last equation and equation (21) yields,

$$\frac{8-6\ln 2}{135}(A-B) = \frac{1}{2}\cdot\frac{1}{135}\left(\frac{476}{9} - \frac{10}{3}\pi^2 + 20\ln^2 2 - \frac{152}{3}\ln 2\right).$$

Thus the relationship between A and B is

$$A - B = \frac{1}{2}\cdot\frac{1}{8-6\ln 2}\left(\frac{476}{9} - \frac{10}{3}\pi^2 + 20\ln^2 2 - \frac{152}{3}\ln 2\right) \approx -0.7185656. \tag{23}$$

We need an additional equation to find the values of A and B. Multiplying (12) by $f\eta^2 d\eta^2$ and integrating over η from zero to one, we obtain the following results for all the terms in (12):

Term 1 on the left-hand side of (12)

$$\int_0^1 f\eta^2 \frac{df}{d\eta} d\eta^2 = \int_0^1 \eta^3 \frac{df^2}{d\eta^2} d\eta^2 = \eta^3 f^2|_0^1 - \int_0^1 f^2 d\eta^3 = -\int_0^1 f^2 d\eta^3.$$

Term 2 on the left-hand side of (12)

$$\int_0^1 \frac{\alpha+1}{5}\eta f\eta^2 d\eta^2 = \frac{\alpha+1}{5}\int_0^1 f\eta^3 d\eta^2.$$

The term on the right-hand side of (12)

$$-\alpha \int_0^1 \int_\eta^1 f(\bar\eta)\bar\eta^2 d\bar\eta d\eta^2 = -\frac{\alpha}{2}\int_0^1 \int_{\eta^2}^1 f(\bar\eta)\bar\eta d\bar\eta^2 d\eta^2$$
$$= -\frac{\alpha}{2}\int_0^1 f(\bar\eta)\bar\eta \left[\int_0^{\bar\eta^2} d\eta^2\right] d\bar\eta^2 = -\frac{\alpha}{2}\int_0^1 f\eta^3 d\eta^2.$$

Combining the above equations results in

$$\int_0^1 f d\eta^3 = \frac{15}{7\alpha+2}\int_0^1 f^2 d\eta^3 + \int_0^1 (1-\eta^2) f d\eta^3. \tag{24}$$

Substituting the first two terms for f from (19) into the right-hand side of the above equation (24) we arrive at

$$\textstyle\int_0^1 f\eta^2\, d\eta \quad \sim \frac{1}{75} + \frac{8-6\ln 2}{135}\alpha\frac{1+A\alpha}{1+B\alpha} \tag{25}$$

where $A = \frac{1}{2}\frac{3047-900\ln^2 2-60\ln 2}{600-450\ln 2}$ and $B = \frac{7}{2}$.

The estimate given by (25) is too large since f^2 behaves as $1/\eta^2$ near $\eta = 0$, while from (18) we know that it behaves as $1/\eta$. The only difference in the equation below from (25) is that when we square the first two terms in (19) which represent f, we drop the α^2 term.

$$\textstyle\int_0^1 f\eta^2\, d\eta \quad \sim \frac{1}{75} + \frac{8-6\ln 2}{135}\alpha\frac{1+A\alpha}{1+B\alpha} \tag{26}$$

where $A = \frac{1}{2}\frac{749-420\ln 2}{200-150\ln 2}$ and $B = \frac{7}{2}$. This expression underestimates the second moment because the coefficient of $1/\eta$ term as $\eta \to 0$ is $\frac{2\alpha}{75}$ while we know from (18) that it should be larger. Equation (23) confirms that the estimate of equation (26) is too low while that of equation (25) is too high. $B - A$ in (26) is too large while it is too low in (25). So we take the geometric average of the A terms in (25) and (26) which should be better

$$\int_0^1 f\eta^2\, d\eta \sim \frac{1}{75} + \frac{8-6\ln 2}{135}\alpha\frac{1+A\alpha}{1+B\alpha} \tag{27}$$

where $A = \frac{1}{2}\sqrt{\frac{3047-900\ln^2 2-60\ln 2}{600-450\ln 2}\cdot\frac{749-420\ln 2}{200-150\ln 2}}$ and $B = \frac{7}{2}$.

One more analytic expression can be obtained by taking $B = \frac{7}{2}$, while A is chosen to satisfy (23). This should provide a better fit for small values of α, since we fit the second moment of f up to the quadratic term in α

$$\int_0^1 f\eta^2\, d\eta \sim \frac{1}{75} + \frac{8-6\ln 2}{135}\alpha\frac{1+A\alpha}{1+B\alpha} \tag{28}$$

where $B = \frac{7}{2}$ and from (23)

$$A = \frac{7}{2} + \frac{1}{2}\cdot\frac{1}{8-6\ln 2}\left(\frac{476}{9} - \frac{10}{3}\pi^2 + 20\ln^2 2 - \frac{152}{3}\ln 2\right).$$

We can obtain one more set of values for A and B by equating the right hand side expression in (22) when $\alpha \to \infty$ with the numerically calculated value of the integral (see Table 1). So we need to solve

$$\lim_{\alpha\to\infty}\left[3\cdot\frac{8-6\ln 2}{135}\cdot\frac{\alpha}{\alpha+1}\cdot\frac{1+A\alpha}{1+B\alpha}\right] = 3\cdot\frac{8-6\ln 2}{135}\cdot\frac{A}{B} = 0.0739.$$

To be consistent with the earlier obtained expressions we take $B = 7/2$ and obtain $A \approx 3.03$. We need to note that unlike the previous approximations for the second moment of f, this last one is semi-analytical in that we need to calculate the integral numerically for the limit $\alpha \to \infty$. After that has been done, the integral for any other values of α is obtained from the right hand side of (22).

2.2. Improved approximations for f. In this section we obtain a new approximation for $f(\eta)$. Using this new approximation and Eqs. (2), (3), (17), we can obtain the value of h and the position of the front r_0. The exact solution for f when $\alpha = 0$ contains $1 - \eta^2$, so we construct approximate solution for f in powers of $(1-\eta^2)$. It will be shown below that the new approximation replicates the exact solution for $\alpha = 0$. In light of equation (18) we operate with f^2 not f. Here we have an expansion of f^2 in powers $(1 - \eta^2)$.

$$(29)\quad f^2 = \left(\frac{\alpha+1}{10}\right)^2 (1-\eta^2)^2 + \frac{\alpha(\alpha+1)}{80}(1-\eta^2)^3 + \frac{\alpha(137\alpha+112)}{11520}(1-\eta^2)^4 + \cdots$$

The above expansion holds for values of η close to 1, while near 0 we have a singularity described by (18). Similar to the cylindrical case treated in [8], for $\alpha = 0$ equation (29) reduces to the exact solution $f = (1 - \eta^2)/10$ as does (14). Our goal is to obtain a uniform approximation for all values of η. We rewrite (29) as

$$(30)\qquad f_1^2 = \sum_{n=1}^{p} Z_n (1-\eta^2)^{n+1}.$$

If $p = 3$, then

$$(31)\qquad Z_1 = \left(\frac{\alpha+1}{10}\right)^2;\ Z_2 = \frac{\alpha(\alpha+1)}{80} \quad \text{and} \quad Z_3 = \frac{\alpha(137\alpha+112)}{11520}.$$

We use a three-term expansion as was done in the cylindrical case [6, 8]. Further terms in the expansion can be obtained if a higher accuracy is desired.

Combining expressions from (30) and (18) we obtain

$$(32)\qquad f^2 \sim f_1^2 + 2\alpha\left[\frac{1}{\eta} - \sum_{n=0}^{m+1} C_n(1-\eta^2)^n\right]\int_0^1 f\eta^2 d\eta,$$

where

$$C_0 = 1,\ C_1 = \frac{1}{2},\ C_2 = \frac{3}{8},\ C_3 = \frac{5}{16},\ C_4 = \frac{35}{128},\ \cdots$$

and $\sum_{n=0}^{m+1} C_n(1-\eta^2)^n$ represents the expansion of $1/\eta$ near $\eta^2 = 1$. The above approximation behaves like equation (18) near $\eta^2 = 0$ for any m. Thus we can hope that this approximation produces sufficiently accurate results for all η. In the next section we compare (32) against the numerical solution.

3. Results

The approximate solution of equation (7) which we obtain through equation (32) depends on the second moment of f. So for comparison purposes we will tabulate several different approaches to calculation of this second moment and afterwards discuss the accuracy of the approximate solution that is obtained from equation (32) using one of these second moments of f.

Table 1 shows $\int f\, d\eta^3/(\alpha+1)$. The integral has been divided by $\alpha + 1$ to obtain a finite limit as $\alpha \to \infty$. In passing, we note that when $\alpha \to \infty$ the power law flux at the origin reduces to an exponential flux: see Appendix B. The table has

TABLE 1. Calculated values of $\frac{\int f\, d\eta^3}{\alpha+1}$ using different methods

	$\alpha = 0.5$	$\alpha = 1$	$\alpha = 1.5$	$\alpha = 2$	$\alpha = 5$	$\alpha \to \infty$
Eq. (27)	0.0539	0.0604	0.0643	0.0669	0.0732	0.0796
Eq. (28)	0.0514	0.0559	0.0584	0.0600	0.0640	0.0678
$A = 3.03$	0.0527	0.0582	0.0614	0.0636	0.0688	0.0739
Numerical	0.0527	0.0583	0.0616	0.0637	0.0689	0.0739

analytical estimates for this normalized integral from equations (27) and (28) for values of $\alpha = 1/2, 1, 1.5, 2, 5, \alpha \to \infty$. A highly accurate numerical calculation of the integral is included for comparison purposes. There is also a semi-analytical entry labeled $A = 3.03$ which depends upon numerical estimates of the limiting value of the integral as $\alpha \to \infty$. However, once this limiting value has been computed this semi-analytical method provides a formula for other choices of α.

We now turn our attention to calculation of the scaling function f. For comparison purposes we obtain a numerical solution of equation (7) to validate our new approximate solutions attained from (32). To achieve this, we rewrite equation (7) as a system of first order ordinary differential equations and use Eqs. (6) and (13) as the initial conditions at $\eta = 1$. To deal with the singularity in the equations at $\eta = 1$ we use (14) to obtain the starting values of f and f' for the numerical calculation. A highly accurate Runge-Kutta-based procedure is then used to obtain numerical values of the scaling function f.

The graphs in Figures 1, 2 and 3 are obtained by using the semi-analytical result for the second moment of f in conjunction with equation (32). Henceforth, we will call this the semi-analytical method. Figure 1 shows the graphs of $f/(\alpha+1)$ obtained using the semi-analytical method for $m = 1, 2$ and 3, as well as $f/(\alpha + 1)$ obtained numerically, and finally $f/(\alpha+1)$ obtained using equation (14) with three terms: in each case $\alpha = 1$. Figure 2 shows the differences of the numerical calculation of $f/(\alpha+1)$ with the semi-analytical method for $\alpha = 1$ and $m = 1, 2, 3$. In contrast to the graphs in Figure 1, the graphs of $f/(\alpha+1)$ in Figure 3 are obtained by varying α and holding m fixed. As the graphs reveal, the quality of these approximate solutions is very good. Finally, we note that upon taking $\alpha = 0$ equation (32) replicates the exact solution.

4. Conclusions

In this article we constructed an approximate similarity solution to a nonlinear diffusion equation with spherical symmetry and a zero initial condition with a flux point source boundary condition. As a result solutions propagate with finite speed and there is a power law singularity at the origin. The resulting approximate scaling function has the same singularity as the true scaling function at the source. While near the front it resembles the Taylor series expansion of the true solution. The combination of these features assures that we have uniform approximation for all values of the similarity variable. Comparison of the approximate solution with a highly accurate numerical solution is favorable. Moreover the approximate solution replicates the known exact solution for one value of the exponent α describing the behavior at the origin.

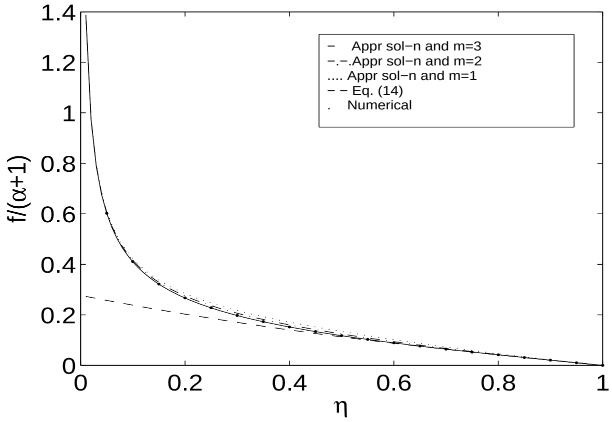

FIGURE 1. Normalized scaling function $f/(\alpha+1)$ versus similarity variable η. Graphs obtained numerically and analytically when $A = 3.03$ ($m = 1$, 2 and 3) and Eq. (14) with three terms. All graphs are for $\alpha = 1$.

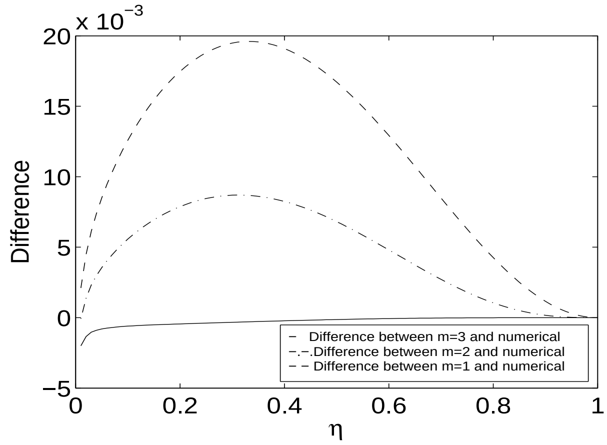

FIGURE 2. Difference between the analytical solutions for different m and the numerical solution. Solid line for $m = 3$, dashed-dotted line for $m = 2$ and dashed line for $m = 1$.

5. Acknowledgements

This work was supported in part by a grant from the University of Nevada Junior Research Grant Fund. This support does not necessarily imply endorsement by the University of research conclusions. Also, this research is supported in part by NSF DMS-0527205. Moreover, this research was supported in part by the Undergraduate Research Award at the University of Nevada, Reno.

6. Appendix A. Expression for $\mathbf{f_2}(\eta)$

Here we provide the expression for $\mathbf{f_2}(\eta)$. To find the terms in the expansion of f in powers of α we use the differential equation (7) and collect terms with the same

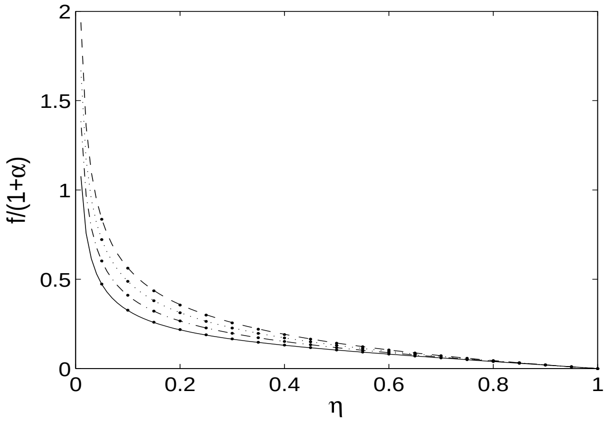

FIGURE 3. Graphs of $f/(1+\alpha)$ versus η obtained numerically and analytically with equation (32) ($m = 3$) for $\alpha = 1/2, 1, 2, 5$. The lowest curve corresponds to $\alpha = 1/2$, next to $\alpha = 1$, etc. Dots represent the numerical solution.

powers of α.
(A.1)

$$\begin{aligned}\mathbf{f_2}(x) &= \frac{8}{15}\left(\frac{1}{1+x}-\frac{1}{2}\right)-\frac{512}{135}\left(\left(-2+\frac{2}{1+x}\right)^{-1}+1\right)\\ &+\frac{112}{45}\frac{1}{1+x}\ln\left(\frac{2}{1+x}\right)\left(-2+\frac{2}{1+x}\right)^{-1}-\frac{32}{45}\left(\left(-2+\frac{2}{1+x}\right)^{-2}-1\right)\\ &-\frac{8}{45}\frac{1}{1+x}\ln\left(\frac{2}{1+x}\right)-\frac{8}{135}\ln\left(\frac{2}{1+x}\right)+\frac{8}{9}\mathrm{dilog}\left(\frac{2}{1+x}\right)\\ &+\frac{8}{45}\ln^2\left(\frac{2}{1+x}\right)+\frac{16}{45}\ln\left(2-\frac{2}{1+x}\right),\end{aligned}$$

where the dilogarithmic function stands for the integral of a special form (e.g. [9]).

7. Appendix B. Limit of large α

Here we illustrate that the limit of the solution as $\alpha \to \infty$ corresponds to an exponential flux at the origin—similar to a result in [2]. We employ the transformation $g = (1+\alpha)f$ and $z = (1+\alpha)\eta$ to modify equation (7):

$$\frac{z}{5}\frac{dg}{dz}-\frac{2\alpha-3}{5(\alpha+1)}g+\frac{1}{z^2}\frac{d}{dz}\left(z^2 g\frac{dg}{dz}\right)=0. \quad \text{(B.1)}$$

Now we consider the solution to equation (1) under the transformations

$$h = A\exp\left(\frac{2kt}{5}\right)g(z) \quad \text{(B.2)}$$

and

$$r = zN\exp\left(\frac{kt}{5}\right), \quad \text{(B.3)}$$

where

$$A = \frac{N^2 k\theta_s}{K_s}. \tag{B.4}$$

As a result equation (1) becomes

$$\frac{1}{5}\eta\frac{dg}{d\eta} - \frac{2}{5}g + \frac{1}{\eta^2}\frac{d}{d\eta}\left(\eta^2 g\frac{dg}{d\eta}\right) = 0. \tag{B.5}$$

Thus as in the case of cylindrical symmetry [8], the above equation implies that in the limit the power-law flux reduces to an exponential flux at the origin.

References

[1] G.I. Barenblatt, On some unsteady-state movements of liquid and gas in porous medium, *Prikl. Mat. i Mekh.*, 16 (1952) 67-78 [in Russian].

[2] G.I. Barenblatt, V.M. Entov and V.M. Ryzhik, *Theory of fluid flows through natural rocks*, Kluwer Academic Publishers, Dordrecht, 1990.

[3] G.I. Barenblatt and M.I. Vishik, On the finite propagation velocity in problems of unsteady-state liquid and gas flow in porous medium, *Prikl. Mat. i Mekh.*, 23 (1956) 411-417 [in Russian].

[4] J. Bear, *Dynamics of fluids in porous media*, American Elsevier Publishing Co., New York, 1972.

[5] J. Crank, *The mathematics of diffusion (2nd edition)*, Oxford University Press Inc., New York, 1975.

[6] E.B. Dussan and F.M. Auzerais, Buoyancy-induced flow in porous-media generated near a drilled oil-well. 1. The accumulation of filtrate at a horizontal impermeable boundary, *J. Fluid Mech.*, 254 (1993) 283-311.

[7] R. Ghez, *Diffusion phenomena*, Kluwer Academic/Plenum Publishers, New York, 2001.

[8] L. Li, D.A. Lockington, M.B. Parlange, F. Stagnitti, D.-S. Jeng, J.S. Selker, A.S. Telyakovskiy, D.A. Barry and J.-Y. Parlange, Similarity solution of axisymmetric flow in porous media, *Adv. Water Resour.*, 28 (2005) 1076-1082.

[9] L. Lewin, *Polylogarithms and associated functions*, North Holland, Amsterdam, 1981.

[10] D.A. Lockington, J.-Y. Parlange, M.B. Parlange and J. Selker, Similarity solution of the Boussinesq equation, *Adv. Water Resour.*, 23 (2000) 725-729.

[11] L.F. Shampine, Some singular concentration dependent diffusion problems, *Z. Angew. Math. Mech.*, 53 (1973) 421-422.

[12] R.E. Smith, K.R. Smettem, P. Broadbridge and D.A. Woolhiser, *Infiltration theory for hydrologic applications*, American Geophysical Union, Washington DC, 2002.

[13] A.S. Telyakovskiy, G.A. Braga and F. Furtado, Approximate similarity solutions to the Boussinesq equation, *Adv. Water Resour.*, 25 (2002) 191-194.

[14] A.S. Telyakovskiy and M.B. Allen, Polynomial approximate solutions to the Boussinesq equation, *Adv. Water Resour.*, 29 (2006) 1767-1779.

[15] Ya.B. Zeldovich and Yu.P. Raizer, *Physics of shock waves and high-temperature hydrodynamic phenomena*, (Ed. W.D. Hayes and R.F. Probstein), Dover Publications Inc, New York, 2002.

Department of Mathematics and Statistics, University of Nevada, Reno, NV 89557, USA
E-mail: jm@unr.edu and olsens3@unr.nevada.edu

Department of Biological and Environmental Engineering, Cornell University, Ithaca, NY 14853, USA
E-mail: jp58@cornell.edu

Department of Mathematics and Statistics, University of Nevada, Reno, NV 89557, USA
E-mail: alekseyt@unr.edu